

FORMATION OF LARGE SCALE STRUCTURE IN THE UNIVERSE

L. Z. FANG

Center for Astrophysics
University of Science and
Technology of China
Hefei, Anhui, China

1. INTRODUCTION

In the universe matter is homogeneously distributed only on very large scale, while on the scale less about a few 100 Mpc matter exists in the form of galaxies, clusters of galaxies and superclusters. Therefore, a fundamental problem in cosmology is to explain why there is large scale inhomogeneities shown by galaxies, clusters of galaxies and superclusters.

Such inhomogeneities can be described mainly by two parameters: the length scale and the amplitude of the density perturbations. The amplitude of the inhomogeneities is defined by

$$\delta = [(\overline{(\rho(x) - \bar{\rho})^2} / \bar{\rho}^2)]^{1/2} \quad (1.1)$$

where $\rho(x)$ is density distribution and $\bar{\rho}$ its mean value. The length scale is given by $\lambda = 2\pi/\bar{k}$, and

$$\bar{k} = \int_0^\infty k |\delta_k|^2 dk / \int_0^\infty |\delta_k|^2 dk \quad (1.2)$$

where δ_k denotes the Fourier component of the perturbed density

namely

$$\delta_k = \int (\rho(x) - \bar{\rho}) e^{ik \cdot x} dx / \bar{\rho} V \quad (1.3)$$

The sketch of large scale inhomogeneity given by visible objects such as galaxies and clusters of galaxies are shown in Table 1.

The clustering of cosmic matter on the scale of galaxies and clusters of galaxies have been studied in great detail. Recently, the progress is to find the evidence of superclusters^[1] and voids^[2]. Inhomogeneity on the scale of superclusters shows up partly as density enhancements, but also as holes, in which the luminous density appears to be practically zero. The existence of large holes is an important characteristic of the universe, because it implies that the large scale density enhancements are not like the inhomogeneity of isolated agglomerations, but like a mesh-structure, i.e. a pattern of connectedness surrounding empty holes.

In the Big-Bang theory it is considered that the inhomogeneity formed from initially very small density perturbations. Therefore, the problems of the formation of large scale structure in the present universe can be expressed as follows: How to form present $\delta \sim 1$ from initial $\delta \ll 1$ of the inhomogeneities with various length scales? When formed such $\delta \sim 1$ for various length scales?

2. CLUSTERING IN AN UNIVERSE WITHOUT MASSIVE IONS

2.1 - Gravitational Instability^[3,4]

The only mechanism to enhance the density fluctuations

in the early universe is gravitational instability, i.e. Jeans instability.

Let us consider an initial inhomogeneity with radius l in a fluid with density ρ , the total mass in this region is about $M \sim \rho l^3$. The time scale of self-gravitational contraction for such an inhomogeneity is then

$$t_g \sim \frac{1}{\sqrt{G\rho}} \quad (2.1)$$

On the other hand, the pressure of the fluid enable the inhomogeneity to produce sound waves. To denote the velocity of sound by v , the time scale of the pressure related process is

$$t_d \sim l/v \quad (2.2)$$

Thus, the initial fluctuations can develop to form a $\delta \sim 1$ inhomogeneity if and only if the following condition can be satisfied

$$t_g \leq t_d \quad (2.3)$$

In the case of

$$t_g > t_d \quad (2.4)$$

the inhomogeneity can not grow, but radiate in the form of waves.

Condition (2.3) can be rewritten as

$$l \geq \lambda_J = v/\sqrt{G\rho} \quad (2.5)$$

or

$$M \geq M_J = v^3/G^{3/2} \rho^{1/2} \quad (2.6)$$

where λ_J and M_J are called, respectively, Jeans length and Jeans mass. Eqs. (2.5) and (2.6) indicate that only the inhomogeneities which have length scale and mass larger, respectively, than the Jeans length and Jeans mass will be able to develop into condensed objects.

In cosmological problems, we are more interested in the mass of baryonic matter than the total mass (baryon plus radiation). We define the Jeans mass of baryon as

$$M_{JB} = \frac{\rho_B}{\rho} M_J \sim \rho_B v^3 / G^{3/2} \rho^{3/2} \quad (2.7)$$

where $\rho = \rho_B + \rho_r$ and ρ_B the baryon density, ρ_r the radiation density.

2.2 - Jeans Mass Before and After the Recombination [3,4]

Now, we calculate the Jeans mass of Baryon in an expanding universe dominated by radiation plus baryons.

Before the recombination epoch, the baryonic density is negligible, we have

$$\rho \sim \rho_r \quad (2.8)$$

and

$$v \sim c \quad (2.9)$$

In an expanding universe, the densities of baryon and radiation as a function of cosmic scale factor R and cosmic temperature T are given by

$$\rho_B \propto R^{-3} \propto T^3 \quad (2.10)$$

$$\rho_R \propto R^{-4} \propto T^4 \quad (2.11)$$

Substituting eqs. (2-8) - (2.11) into eq. (2.7), one finds

$$M_{JB} \propto T^{-3} \quad (2.12)$$

At the time of recombination, namely $T \sim 4000$ K, the baryonic density is about the same as that of radiation

$$\rho_B \sim \rho_R \quad (2.13)$$

and ρ_R can be derived from its present value $\rho_{R0} = 4 \times 10^{-34} \text{ gm/cm}^3$ by

$$\rho_R \sim \rho_{R0} (4000/2.7)^4 \quad (2.14)$$

From Eqs. (2.13) and (2.14), one obtains the Jeans mass at the recombination epoch as

$$M_{JB} \sim 10^{19} M_{\odot} \quad (2.15)$$

Therefore, before the recombination we have

$$M_{JB} \sim 10^{19} \left(\frac{T}{4000}\right)^{-3} \quad (2.16)$$

During the recombination, radiation starts to decouple with baryon, the velocity v in Eq. (2.7) drops from c (Eq. (2.9)) to

$$v_B \sim (k \cdot 4000 / m_p)^{1/2} \quad (2.17)$$

where k is the Boltzmann constant and m_p proton mass. Since $M_{JB} \propto v^3$ the value of M_{JB} should drop by a factor of

$$\left(\frac{v_B}{c}\right) \sim 10^{-12} \quad (2.18)$$

So just after the recombination, the Jeans mass is

$$M_J \sim 10^{19} \cdot 10^{-12} \sim 10^7 M_\odot \quad (2.19)$$

After the recombination, the expansion of matter in the universe is adiabatic, namely

$$T_m \propto V^{-(\gamma-1)} \quad (2.20)$$

where T_m is the temperature of baryonic matter, $V \sim R^3$ is comoving volume and γ the specific heat ratio. Since baryonic matter consist mainly of hydrogen and helium, we have $\gamma = 5/3$. One find then

$$T_m \propto T^2 \quad (2.21)$$

or

$$v \propto T \quad (2.22)$$

Substituting Eqs. (2.11) and (2.22) into (2.7), we obtain

$$M_{JB} \propto T^{3/2} \quad (2.23)$$

Considering Eq. (2.19) one got finally

$$M_{JB} \sim 10^7 \left(\frac{T}{4000}\right)^{3/2} \quad (2.24)$$

The behaviour of the Jeans mass as a function of T is shown in Fig. 1. From this result, it can be found easily that an initial inhomogeneity with the scale about the same as or less than that of superclusters can contract only after the recombination, namely, all present-observed structure in the universe can be formed only in the period of after recombination.

Moreover, no characteristic mass of about $10^{12} M_{\odot}$, $10^{14} M_{\odot}$ and $10^{15} M_{\odot}$ are shown in the Jeans mass given by Eq. (2.16) and (2.24).

2.3 - Growth of Perturbations After the Recombination^[4]

We consider the growth of a perturbation with length scale much larger than the Jeans length. In this case the matter in the universe can be described as a pressureless dust and the dynamics of expansion of the universe is described by

$$\frac{\ddot{R}}{R} = - \frac{4\pi}{3} G \rho_B \quad (2.25)$$

$$\rho_B R^3 = \text{const.} \quad (2.26)$$

The solution of Eqs. (2.25) and (2.26) is

$$R \propto t^{2/3} \quad (2.27)$$

It can be found from Eqs. (2.25) and (2.26) that in linear approximation the perturbations $\delta\rho_B$ and δR should satisfy the following equations

$$\begin{aligned} \frac{\delta\rho_B}{\rho} &= - 3 \frac{\delta R}{R} \\ \delta\ddot{R} &= - \frac{4\pi}{3} G [R\delta\rho_B + \rho\delta R] \end{aligned} \quad (2.28)$$

which have a growth solution as

$$\delta \equiv \frac{\delta\rho_B}{\rho_B} \propto t^{2/3} \propto R \propto T^{-1} \quad (2.29)$$

According to Table 1, at present time the amplitudes of

Inhomogeneities with length scale less than a hundred Mpc are, at least, larger than unity, i.e.

$$\delta_0 \geq 1 \quad (2.30)$$

Therefore, the inhomogeneities at the recombination epoch should have

$$\delta \sim \delta_0 \left(\frac{T_0}{4000} \right) \geq 10^{-3} \quad (2.31)$$

2.4 - Isothermal and Adiabatic Fluctuations

The initial fluctuations can be divided into two sort: isothermal and adiabatic. In the case of isothermal fluctuation the inhomogeneity exists only in the baryonic component, while the radiation component distributes uniformly, namely

$$T = \text{const.} \quad (2.32)$$

In the case of adiabatic fluctuation both baryon and radiation components distribute inhomogeneously, while the ratio between the number densities of photons and baryons, n_T and n_B , are the same everywhere, namely

$$n_T/n_B = \text{const.} \quad (2.33)$$

$$\delta = \frac{\delta \rho_B}{\rho_B} = \frac{\delta n_B}{n_B} = \frac{\delta n_T}{n_T} = 3 \frac{\delta T}{T} \quad (2.34)$$

Recently, theories of the inflationary universe and baryosynthesis show that the primordial density fluctuations in

the very early universe should be adiabatic^[5]. Therefore, from Eqs. (2.31) and (2.34) we find

$$\frac{\delta T}{T} \geq \frac{1}{3} \times 10^{-3} \quad (2.35)$$

Obviously, this result is inconsistent with the observations of anisotropy of the background radiation, it is^[6]

$$\frac{\delta T}{T} \leq 10^{-4} \quad (2.36)$$

in a word, Eqs. (2.35) and (2.36) seem to show that there is not enough time, after the recombination, to form the present observed structure from initially adiabatic perturbations.

3. DARK MATTER AND ITS DISTRIBUTION

3.1 - Evidence for Dark Matter Dominant Universe

The difficulty mentioned in the last section might be overcome if the universe is not dominated by radiation plus baryons but by non-baryonic dark matter such as massive ions, namely, the total density ρ in the universe is given by

$$\rho = \rho_1 + \rho_2 \quad (3.1)$$

where ρ_1 and ρ_2 denote, respectively, the densities of radiation plus baryons and dark matter, and

$$\rho_1 \ll \rho_2 \quad (3.2)$$

That the most of the mass in the universe may be invisible has been studied for a long time. Many evidences for the existence of dark matter as the dominant component in the universe have been found.

The first evidence is that the rotation curves of spiral galaxies are flat^[7]. It means that the mass within radius r is proportional to r . On the other hand, the optical luminosity is well known to drop exponentially with scale-length (e-folding) of $0.1 \times$ Holmberg diameter. Therefore, the flatness of rotation curves show the total mass of spiral galaxies are dominated by their invisible halos.

The second evidence is the mass-to-light ratio M/L for groups and clusters of galaxies are much higher than for single galaxies. M/L increases with the linear size of the system considered and it appears to increase some 50-fold as we go from the kpc-sized single galaxies to the Mpc-sized Abel clusters^[8]. This means that only a small fraction of the mass of a cluster is in the form of luminous galaxies, but the major fraction is dark.

The third evidence come from the systematic difference in the determination of q_0 ^[9]. The Hubble diagram method to determine q_0 always gives $q_0 > 1/2$, while the mean mass density method always gives $q_0 < 1/2$. Therefore, the main reason for this disagreement may not be the coarseness or insufficiency of data; rather it is due to the different hypotheses underlying the different methods. In the Hubble diagram method, one assumed no evolution in luminosity of galaxies or quasars, while in the mean mass density method one assumed that all matter is concentrated in, or distributed proportionally to, galaxies, clusters or local superclusters and that there does not exist dark matter with

different distribution from galaxies. One of the probable ways out of the disagreement is then that there exists dark matter in the universe.

A theoretical argument in favour of dark matter is given by the inflationary universe. If there was a inflation stage in the very early universe due to Higgs phase transition, the present density should be equal to^[10]

$$\rho_c = 3H_0^2/8\pi G = 1.9 \times 10^{-29} h^2 \text{ g cm}^{-3} \quad (3.3)$$

where H_0 is the Hubble constant and

$$h = H_0/100 \text{ km s}^{-1} \text{ Mpc}^{-1} \quad (3.4)$$

ρ_c is much larger than the density of galactic component, ρ_G namely

$$\rho_G \leq 0.2 \rho_c \quad (3.5)$$

3.2 - Distribution of Dark Matter^[11]

In a dark matter dominant universe, the information of distribution of dark matter is necessary in studying the formation of large scale structure, because the total density inhomogeneity should be dominated by the density distribution of dark matter. Obviously, it is more difficult to determine the length scale and the amplitude of the inhomogeneity of the dark matter than that of visible objects. Nevertheless, some information of such inhomogeneity can be found by their gravitational effect.

Let us consider the local supercluster. Its centre is the Virgo cluster, and the local group, located some $10 h^{-1} \text{Mpc}$ away, is a member. On such a scale, the Hubble velocity is the dominant term and we can find a relation of the deviation from Hubble flow with density enhancement. Consider a spherically symmetric mass enhancement δM . The additional acceleration g at a distance D from its centre is

$$g = G\delta M/D^2 = (4\pi/3)GD\delta\rho \quad (3.6)$$

where $\delta\rho$ is the mean density enhancement within D . Substituting (3.3) into (3.6) gives

$$g = H_0 \Omega V \delta\rho/2\rho \quad (3.7)$$

where

$$\Omega = \rho/\rho_c \quad (3.8)$$

and

$$V = H_0 D \quad (3.9)$$

is the Hubble velocity at D . The accumulated peculiar velocity in one Hubble time is

$$v = g H_0^{-1} \quad (3.10)$$

From Eqs. (3.7) and (3.10) we then have

$$\Omega = 2(v/V)/\delta \quad (3.11)$$

where $\delta = \delta\rho/\rho$.

The peculiar velocity v of the local group in the direction of the Virgo cluster has been determined by a number of authors^[12], it is about 300 km/s. With the Hubble velocity of the local group with respect to the Virgo cluster,

$V = 1050 \text{ km/s}^{[13]}$, we find from eq. (3.11) and $\Omega = 1$ that

$$\delta \sim 0.6 \quad (3.12)$$

However, Yahil et al. found that the amplitude of galactic inhomogeneity in the local supercluster is^[14]

$$\delta_G \sim 3.5 \quad (3.13)$$

This means that the density distribution of dark matter is more uniform than galaxies.

Now we take a statistical viewpoint on the distribution of matter. The entire galactic population is regarded as a field of fluctuating density in random motion with respect to the Hubble flow. One can find a relation between the potential energy in the density fluctuations W and the kinetic energy of the peculiar velocity T as follows^[15,16]

$$T = -\beta W \quad (3.14)$$

where $\beta = \frac{1}{2}, \frac{2}{3}$ or $\frac{4}{7}$, and

$$T = 3 v^2/2 \quad (3.15)$$

$$W = -2\pi G\rho \int r \xi(r) dr$$

where $\xi(r)$ is the two-point correlation function. Using again Eqs. (3.3) and (3.8) we have

$$\Omega = \frac{2}{\beta} (v^2/H_0^2)/U \quad (3.16)$$

where

$$U = \int r \xi(r) dr \quad (3.17)$$

It should be emphasized that the correlation function in (3.17) is of total density distribution. If we assume that the correlation

function of total mass density is the same as that of galaxies

$$U = U_G \quad (3.18)$$

we found^[17]

$$\Omega = 0.2 \ll 1 \quad (3.19)$$

Therefore, $\Omega = 1$ implies

$$U \ll U_G \quad (3.20)$$

Thus, the result from the statistical approach is in agreement with those from the local supercluster, namely,

$$\delta \ll \delta_G \quad (3.21)$$

3.3 - Upper Limit for the Inhomogeneity of Dark Matter

An upper limit to the amplitude of the inhomogeneity of dark matter can be found by the gravitational deflection of density inhomogeneity^[18,19].

The propagation of radiation will be affected by the metric perturbation of density inhomogeneity, so the intensity fluctuation will be caused by the stochastic small gravitational deflection. It is analogous to the scintillation of light signal caused by a refractive medium with statistically distributed inhomogeneity. This effect is observable as a luminosity difference between sources with angular distance of the order of

$$\theta_s \sim \lambda/d \quad (3.22)$$

where d is the distance of the sources and λ is the length scale

of the inhomogeneity. The light signals from the source have experienced a statistically independent stochastic field if their arriving directions are different. The luminosity fluctuations are caused from these different histories of the propagation.

The mean square fluctuation of intensity is given by

$$\left(\frac{\Delta I}{I}\right)^2 = \frac{2}{3} Q d^3 \quad (3.23)$$

and

$$Q = 2 \overline{h^2} \int_0^\infty \left[\frac{1}{r^2} \frac{d^2}{dr^2} M(r) - \frac{1}{r^3} \frac{d}{dr} M(r) \right] dr \quad (3.24)$$

$\overline{h^2}$ and $M(r)$ can be expressed by the density perturbation spectrum δ_k as follows:

$$\overline{h^2} = \left(\frac{6\pi G\rho}{c^2}\right)^2 \overline{k^{-4}} \delta^2 \quad (3.25)$$

$$M(r) = \int_0^\infty dk k^{-3} |\delta_k|^2 \sin kr / \int_0^\infty dk k^{-2} |\delta_k|^2 r \quad (3.26)$$

where $\overline{k^{-4}}$ is the average of k^{-4} over the $|\delta_k|^2$.

As an example, we take

$$|\delta_k|^2 = A k^4 \exp \{-(k/k)^2\} \quad (3.27)$$

which is the constant curvature spectrum with out off near the average of k . Using eq. (3.27), one find

$$\overline{h^2} = \frac{4}{15} \left(\frac{6\pi G\rho}{c^2}\right)^2 \frac{\delta^2}{k^4} \quad (3.28)$$

and

$$M(r) = \exp \{-(kr)^2/4\} \quad (3.29)$$

Then, the relation (3.23) gives

$$\left(\frac{\Delta I}{I}\right)^2 = \frac{4\sqrt{\pi}}{45} \left(\frac{6\pi G\rho}{c^2}\right)^2 \frac{d^3}{k} \delta^2 \quad (3.30)$$

For sources with redshifts larger than about 2, we have

$$x \sim c/H_0 \sim c/(G\rho/\Omega)^{1/2} \quad (3.31)$$

Using eqs. (3.3), (3.8) and (3.31), the relation (3.30) gives

$$\frac{\Delta I}{I} \sim \Omega^{1/2} \frac{\lambda}{c/H_0} \delta \quad (3.32)$$

or

$$\delta < 1 \times \lambda_{10}^{-1/2} h^{-1/2} \Omega^{-1} \left(\frac{\Delta I}{I}\right)_{-1} \quad (3.33)$$

where $\lambda_{10} = \lambda/10$ Mpc and $\left(\frac{\Delta I}{I}\right)_{-1} = \left(\frac{\Delta I}{I}\right)/10^{-1}$.

Recently, several homogeneous search for quasars have been made. It is found that the difference of mean luminosities of sources located at different directions are not larger than 10% [20]. Therefore, from (3.33) we find an upper limit to δ . This result is shown in Fig. 2. It denotes the amplitudes of the total density inhomogeneity are less than that of galaxies by a factor 3 - 5.

Therefore, a new problem in the dark matter dominant universe is: how are the difference in the distribution of visible objects and dark matter form? why does the visible objects cluster, specially on the scale less than superclusters, while dark matter has up to now remained rather uniform on such scale? Before to find an answer to this problem, we should first stude the clustering in an universe containing two- or multi-

4. CLUSTERING IN A TWO- OR MULTI-COMPONENT SYSTEM

4.1 - Clustering Feature in a Two-component System [21]

Let us consider a self-gravitational system containing two components of matter, taking $\bar{\rho}_1$, $\bar{\rho}_2$ and \bar{v}_1 , \bar{v}_2 to denote, respectively, the densities and the velocity dispersions of 1 and 2 in the uniform ground state. The two components interact with each other only through gravitation.

The clustering in such a system have been studies by several authors. The only case to be discussed by Guyot and Zeldovich [22] is an open universe with comparable density of radiation and matter, which is different from the case of $\bar{\rho}_1 \ll \bar{\rho}_2$ we want to discuss. Meszaros investigated [23] the behaviour of point masses embedded in a smooth, expanding cosmological substratum. The main conclusion of his research is that the perturbations of particle component cannot grow as long as the density of particle component is less than that of substratum, namely, whether clustering is able to occur in a two-component system depends completely on the dominant component. However, this result is not correct due to the assumption used in his analysis that the density of substratum is always equal to the unperturbation value, in fact, both components can be perturbed during clustering.

Clustering feature can be described clearly by the time scales of response to density perturbations as that of (2.1) and

(2.2). In a two-component system there are four relevant time scale with respect to a density perturbation of length scale ℓ [24], namely, two damping times defined by

$$t_{d1} \sim \ell/\bar{v}_1, \quad t_{d2} \sim \ell/\bar{v}_2 \quad (4.1)$$

and two growing times defined by

$$t_{g1} \sim (G\bar{\rho}_1)^{-1/2}, \quad t_{g2} \sim (G\bar{\rho}_2)^{-1/2} \quad (4.2)$$

The Jeans lengths λ_{J1} and λ_{J2} of components 1 and 2 are determined by the following conditions, respectively,

$$t_{g1} \sim t_{d1}, \quad t_{g2} \sim t_{d2} \quad (4.3)$$

According to the relationship between the time scales, the responses to perturbations can be divided into the following cases:

a) growth in both components

$$t_{g1} < t_{d1}, \quad t_{g2} < t_{d2} \quad (4.4)$$

b) damping in both components

$$t_{g1} > t_{d1}, \quad t_{g2} > t_{d2} \quad (4.5)$$

c) growth in 1, but damping in 2

$$t_{g1} < t_{d1}, \quad t_{g1}, t_{g2} > t_{d2} \quad (4.6)$$

in this case the damping time of 2 is less than the growing time in both 1 and 2.

d) growth in 2, but damping in 1

$$t_{g2} < t_{d2} \quad , \quad t_{g2}, t_{g1} > t_{d1} \quad (4.7)$$

e) growth in 1, slow growth in 2

$$t_{g1} < t_{d1} \quad , \quad t_{d2} > t_{g2} \gg t_{d1} \quad (4.8)$$

in this case the perturbation can arise growing response in 2, while it is very small compared to that in 1 due to the growing time of 1 which is very large.

f) growth in 2, slow growth in 1

$$t_{g2} < t_{d2} \quad , \quad t_{d1} > t_{g1} \gg t_{d2} \quad (4.9)$$

From these criteria, one can find that if the two components of matter satisfy the following conditions

$$\bar{\rho}_1 \ll \bar{\rho}_2 \quad , \quad \lambda_{J1} \ll \lambda_{J2} \quad (4.10)$$

i.e.

$$t_{g1} \gg t_{g2} \quad , \quad t_{d1} \gg t_{d2} \quad (4.11)$$

the response to a perturbation belongs to the case c for length scale $\ell \sim \lambda_{J1}$ and to the case f for $\ell \sim \lambda_{J2}$. Therefore, under the condition (4.10), a significant inhomogeneity with the scale of about λ_{J1} can be form in the non-dominant component 1, but not in the dominant component. This show that the clustering in a two component system is not determined only by the dominant component.

4.2 - Jeans Length of a Two-component Fluid [25]

The fundamental equations for a non-relativistic and non-expansive self-gravitational two-component fluid are

Component 1

$$\begin{aligned} \frac{\partial \rho_1}{\partial t} + \nabla \cdot (\rho_1 \vec{v}_1) &= 0 \\ \frac{\partial \vec{v}_1}{\partial t} + (\vec{v}_1 \cdot \nabla) \vec{v}_1 &= - \frac{1}{\rho_1} \nabla p_1 + \vec{g} \end{aligned} \quad (4.12)$$

Component 2

$$\begin{aligned} \frac{\partial \rho_2}{\partial t} + \nabla \cdot (\rho_2 \vec{v}_2) &= 0 \\ \frac{\partial \vec{v}_2}{\partial t} + (\vec{v}_2 \cdot \nabla) \vec{v}_2 &= - \frac{1}{\rho_2} \nabla p_2 + \vec{g} \end{aligned} \quad (4.13)$$

gravitational field

$$\begin{aligned} \nabla \times \vec{g} &= 0 \\ \nabla \cdot \vec{g} &= - 4\pi G(\rho_1 + \rho_2) \end{aligned} \quad (4.14)$$

From eqs. (4.12) - (4.14), one can find its dispersion relation for linear perturbations with wave number k and frequency ω as follows:

$$\begin{aligned} \omega^4 - \omega^2 [k^2 (\bar{v}_1^2 + \bar{v}_2^2) - 4\pi G(\bar{\rho}_1 + \bar{\rho}_2)] \\ + k^4 \bar{v}_1^2 \bar{v}_2^2 - 4\pi Gk^2 (\bar{\rho}_1 \bar{v}_2^2 - \bar{\rho}_2 \bar{v}_1^2) &= 0 \end{aligned} \quad (4.15)$$

It is easy to show from (4.15) that the necessary and sufficient condition for the onset of Jeans instability is

$$k^2 \leq 4\pi G \left(\frac{\bar{\rho}_1}{\bar{v}_1^2} + \frac{\bar{\rho}_2}{\bar{v}_2^2} \right) \quad (4.16)$$

In other words, the Jeans length λ_J is

$$\frac{1}{\lambda_J^2} = \frac{1}{\lambda_{J1}^2} + \frac{1}{\lambda_{J2}^2} \quad (4.17)$$

where $\lambda_{J1}^2 = \bar{v}_1^2 / G\bar{\rho}_1$, $\lambda_{J2}^2 = \bar{v}_2^2 / G\bar{\rho}_2$ are, respectively, the Jeans lengths of the two components. From eq. (4.17) one finds that under the conditions of (4.10) the Jeans length of the whole system is not determined by the dominant component, but by the non-dominant one.

4.3 - Clustering in an Expanding Two-component Universe [21]

In linear theory of the evolution of inhomogeneity growth or damping for a perturbation can be described by development matrix $D_{ij}(k,t)$ defined, for a two-component system, by

$$\begin{bmatrix} \delta_{1k}(t) \\ \delta_{2k}(t) \end{bmatrix} = \begin{bmatrix} D_{11}(k,t) & D_{12}(k,t) \\ D_{21}(k,t) & D_{22}(k,t) \end{bmatrix} \begin{bmatrix} \delta_{1k}(0) \\ \delta_{2k}(0) \end{bmatrix} \quad (4.18)$$

where $\delta_{ik} = (\delta\rho/\rho)_{ik}$ are the amplitudes of inhomogeneity with scale $\ell = 2\pi/k$ in component i .

As an example we calculated the development matrix for an expanding universe with two components of matter, dominant one is collisionless gas, non-dominant one is fluid. The method used in this calculation is the same as Gilbert [26]. The equations describing the development of perturbation are

$$\frac{d^2 \delta_{1k}}{dS^2} + R \left(\frac{\bar{\rho}_1}{\bar{\rho}_2} \right) \left(\frac{\lambda_{J1}^2 k^2}{R^2} - 1 \right) \delta_{1k} = R \delta_{2k} \quad (4.19)$$

$$\begin{aligned} \delta_{2k}(S) - \int_0^S R(S') \phi[k(S-S')] (S-S') \delta_{2k}(S') dS' &= \\ &= \int_0^S R(S') \phi[k(S-S')] (S-S') \left(\frac{\bar{\rho}_1}{\bar{\rho}_2} \right) \delta_{1k}(S') dS' + \phi(kS) \delta_{2k}(0) \end{aligned} \quad (4.20)$$

where R is the cosmic scale factor, S is the conformal time in the Newtonian cosmology defined by $dS = dt/R^2$, and function ϕ is determined by the ground state distribution function of component 2

$$\phi(k) = \frac{1}{\bar{\rho}_2} \int f_2^{(0)} e^{-2\pi i \vec{k} \cdot \vec{Z}} d\vec{Z} \quad (4.21)$$

where \vec{Z} is the velocity in the comoving coordinate.

The results for the development matrix are shown in Figs. 3 and 4, in which we take $f_2^{(0)}$ as

$$f_2^{(0)} = 1/[\exp(Z/v_2) + 1] \quad (4.22)$$

the relevant parameters are taken as

$$\bar{\rho}_1/\bar{\rho}_2 = 0.1 \quad (4.23)$$

$$\lambda_{J1}/\lambda_{J2} = 0.1$$

Fig. 3 shows the evolution of inhomogeneity amplitudes δ_{1k} and δ_{2k} , initial perturbation are $\delta_{1k} = 1$ and $\delta_{2k} = 0$, and Fig. 4 shows the case of initial conditions $\delta_{1k} = 0$ and $\delta_{2k} = 1$. In Figs. 3 and 4, t is in units of $(4\pi G \bar{\rho}_2)^{-1/2}$ and k in $2\pi/\lambda_{J2}$.

It can be seen from Figs. 3 and 4 that in the beginning stage the perturbation of $k > 1$, i.e. $\lambda < \lambda_{J2}$, are growing only in 1, but damped in 2. The amplitudes of developed inhomogeneities always satisfy the following relations

$$\delta_{1k}(t) > \delta_{2k}(t) \quad (4.24)$$

for $k > 1$, and

$$\delta_{1k}(t) \sim \delta_{2k}(t) \quad (4.25)$$

for $k \leq 1$.

The evolution of spectrum of inhomogeneity are shown in Figs. 5 and 6. In Fig. 5 the initial perturbations are taken as a white noise spectrum in 1 and no perturbation in 2, i.e.

$\delta_{1k}(0) = 1$, $\delta_{2k}(0) = 0$. In Fig. 6, it is $\delta_{2k}(0) = 1$, $\delta_{1k}(0) = 0$.

It can be found from Figs. 5 and 6 that the clustering of non-dominant component on the scales less than λ_{J2} are always larger than that of dominant component, regardless of whether the initial perturbations exist in dominant or in non-dominant components, namely, the dispersion process in the dominant component can not erase all the perturbations with scales less than λ_{J2} , which still can carry on or develop in the non-dominant component.

Above-mentioned results do not depend on the detail of dispersion mechanism of the considered matter, but only on the condition (4.10). For instance, if we take both components to be collisionless gas or to be fluid, the conclusion is the same as above.

In a word, it is possible to form smaller scale structure in the non-dominant component, more strongly and more earlier than in the dominant component of a two component universe.

5. COMPOSITION OF DARK MATTER AND CLUSTERING SCENARIO

5.1 - Preferential Clustering in Neutrino Dominant Universe [27]

The number density of neutrino after the e^+e^- annihilation is

$$n_\nu = (3/22)n_\gamma g_\nu = 54.5 g_\nu \text{ cm}^{-3} \quad (5.1)$$

where g_ν denotes the number of spin states of neutrino (ν and $\bar{\nu}$ also as two different spin states). There may be 3 types of neutrinos, ν_e , ν_μ and ν_τ , so we have $g_\nu = 6$ for 2-component neutrinos. Hence just as photon, the neutrino number density would also be larger than baryon number density by a factor of $n^{-1} = \frac{n_B}{n_\nu} \sim 10^9$. Therefore, neutrinos will become the dominant component in the universe if its rest mass m is about or larger than a few eV.

After the decoupling of neutrinos and e^+e^- annihilation, neutrino distribution function in momentum space is

$$dn_\nu = \frac{4\pi}{(2\pi\hbar)^3} g_\nu p^2 dp \{ \exp(pc/0.71kT) + 1 \}^{-1} \quad (5.2)$$

From eq. (5.2) we can derive the mean square speed as follows

$$v_\nu^2 = 4.8 \times 10^{-4} c^2 \left(\frac{m_\nu}{30\text{eV}} \right)^{-2} \left(\frac{T}{4000} \right)^2 \quad (5.3)$$

Hence we obtain the Jeans length and Jeans mass as

$$\lambda_{J\nu} = 6.2 \times 10^3 \left(\frac{g_\nu}{6} \right)^{-1/2} \left(\frac{m_\nu}{30} \right)^{-3/2} \left(\frac{T}{4000} \right)^{-1/2}, \text{ pc} \quad (5.4)$$

$$M_{J\nu} = 8.1 \times 10^{14} \left(\frac{g_\nu}{6} \right)^{-1/2} \left(\frac{m_\nu}{30} \right)^{-7/2} \left(\frac{T}{4000} \right)^{3/2} M_\odot \quad (5.5)$$

here we already assumed $m_{\nu_e} = m_{\nu_\mu} = m_{\nu_\tau} \equiv m_\nu$. $M_{J\nu}$ and $\lambda_{J\nu}$ have been drawn in Figs. 1 and 7. From Fig. 7 we see $\lambda_{J\nu} \ll \lambda_{JB}$ before the recombination, therefore, by using (4.17), we know that at that time the Jeans mass and length depend only on neutrinos.

On the other hand, an upper mass limit for neutrino clustering given by cosmic horizon is

$$M_{h\nu} \approx \frac{4}{3} \pi n_\nu m_\nu \lambda_h^3 \quad (5.6)$$

where $\lambda_h \sim ct$ and

$$t = \frac{2}{3H_0} \left(\frac{2.7}{T}\right)^{3/2} \quad (5.7)$$

Taking $H_0 = 75 \text{ km s}^{-1} \text{ Mpc}^{-1}$, we have

$$M_{h\nu} = 3.6 \times 10^{17} \left(\frac{g_\nu}{6}\right) \left(\frac{m_\nu}{30}\right) \left(\frac{T}{4000}\right)^{-3/2} M_\odot \quad (5.8)$$

From Eqs. (5.5) and (5.8), we can find a characteristic temperature T_1 by $M_{J\nu} = M_{h\nu}$, it is

$$T_1 = 3 \times 10^4 \left(\frac{g_\nu}{6}\right)^{1/2} \left(\frac{m_\nu}{30}\right)^{3/2} \text{ K} \quad (5.9)$$

T_1 is the temperature, at which the cosmic neutrinos can first begin to cluster during the expansion of the universe.

Substituting (5.9) into (5.4) and (5.5), we obtain the Jeans length and mass at T_1

$$\lambda_{\nu 1} = 2.3 \times 10^3 \left(\frac{g_\nu}{6}\right)^{-3/4} \left(\frac{m_\nu}{30}\right)^{-9/4} \text{ pc} \quad (5.10)$$

$$M_{\nu 1} = 1.7 \times 10^{16} \left(\frac{g_\nu}{6}\right)^{1/4} \left(\frac{m_\nu}{30}\right)^{-5/4} M_\odot \quad (5.11)$$

$\lambda_{\nu 1}$ and $M_{\nu 1}$ give the length and mass scale of earliest one to

become jeans instable in the early universe. So, we called λ_{v1} and M_{v1} as preferential clustering length and mass, respectively [25].

Since T_1 is larger than the temperature of recombination, the onset of the Jeans instability before the recombination is possible. Since $T_1/2.7 \sim 10^{-4}$, an initial perturbation of $\delta \sim 10^{-4}$ at T_1 can form the present structure of $\delta \sim 1$.

Obviously, due to the preferential clustering, the amplitudes of the massive neutrino inhomogeneity at the recombination should be $\delta \geq 10^{-3}$. In this case we need to discuss the influence of non-uniform distribution of massive neutrinos on the anisotropy of the microwave background. Because there are no coupling between neutrinos and photons except for gravitational interaction, the main influence of massive neutrinos comes from their gravitational potential, which gives an additional fluctuation in the background by gravitational redshift effect. We may estimate this redshift as

$$\delta Z \sim G(\ell_v^3 \delta \rho_v) / \ell_v c^2 \quad (5.12)$$

where ℓ_v is the radius of the neutrino disturbance region at the recombination

$$\ell_v \sim \lambda_{v1} \left(\frac{T_1}{4000} \right) \quad (5.13)$$

This redshift would give rise to anisotropy in the background radiation by an order of

$$\frac{\delta T}{T} \sim \delta Z \sim 0.04 \Omega \delta_v \quad (5.14)$$

Therefore, for consisting with (2.36) and $\Omega = 1$, we should have

$$\delta_{\nu} \leq 3 \times 10^{-3}$$

(5.15)

where $\delta_{\nu} = \delta\rho_{\nu}/\rho_{\nu}$. (5.15) is a limitation to the inhomogeneity of massive neutrinos at the recombination. Comparing (5.15) with (2.31), one can conclude that the preferential clustering mechanism provide a way to overcome the difficulty mentioned in the end of the section 2.

5.2 - Problems in Neutrino Dominant Universe

Another advantage of the neutrino dominant universe is to provide a natural interpretation for the formation of clusters of galaxies. The preferential mass of neutrinos (5.11) multiplied by the density ratio of baryons to neutrinos at the epoch of recombination would represent the preferential clustering mass of baryonic component, it is

$$M = M_{\nu 1} \left(\frac{\rho_B}{\rho_{\nu}}\right) = 3.2 \times 10^{14} \left(\frac{n}{5 \times 10^{-10}}\right) \left(\frac{g_{\nu}}{6}\right)^{-3/4} \left(\frac{m_{\nu}}{30}\right)^{-9/4} M_{\odot} \quad (5.16)$$

which is just of the order of clusters of galaxies. During the perturbations develop and collapse, there must leave behind some large empty regions or voids. Evidently, the size of these voids may just be measured by the preferential length in the comoving sense, namely

$$\begin{aligned} l &\sim \lambda_{\nu 1} (T_1/T) \\ &= 25(1+z)^{-1} \left(\frac{g_{\nu}}{6}\right)^{-1/4} \left(\frac{m_{\nu}}{30}\right)^{-3/4} \text{ Mpc} \end{aligned} \quad (5.17)$$

z is the redshift corresponding to the distance of the void.

The observed scale of the voids is about 40 - 100 Mpc, agreeing well with the estimation of (5.17).

In a word, the observed distribution of galaxies, especially the filamentary structure with scale of 100 Mpc, can be explained naturally in the massive neutrino dominant universe. However, a serious problem is that the formation time of such structure is too late. Several numerical simulations found that the large scale structure collapses only after $z \sim 2$ [18,29]. On the other hand, since the initial fluctuations are adiabatic, the formation of structure on smaller scales should occur after the large scale structure. Therefore, in the neutrino dominant universe, the redshifts of all the small scale objects should be less than 2. Obviously, it is inconsistent with the existence of objects with redshifts larger than 2. Thus, in the neutrino dominant universe we need to explain how to form small scale objects before the large one.

The second problem is on the distributions of visible objects and of dark matter. As pointed out in the section 3, the visible objects in the universe are clustered on the scales of galaxies, clusters of galaxies and superclusters, while dark matter distributed rather uniformly at least on the scales of less than that of superclusters. It seems possible to explain this character by the mechanism discussed in 4.3. In the neutrino dominant universe, the density ratio of baryons ρ_B to massive neutrinos ρ_ν is

$$\rho_B/\rho_\nu \approx 1.9 \times 10^{-2} \left(\frac{g_\nu}{6}\right)^{-1} \left(\frac{m_\nu}{30}\right)^{-1} \left(\frac{n_{10}}{5}\right)^{-1/2} \quad (5.18)$$

where $n_{10} = n_B/n_\nu \times 10^{10}$ denotes the number ratio of baryons to

photons in background. After the recombination the ratio of Jeans lengths of baryons λ_{JB} to massive neutrinos $\lambda_{J\nu}$ is given by

$$\lambda_{JB}/\lambda_{J\nu} \approx 0.86 \times 10^{-2} \left(\frac{m_{\nu}}{30}\right)^{3/2} \left(\frac{n_{10}}{5}\right)^{-1/2} \quad (5.19)$$

Eqs. (5.18) and (5.19) are just in accord with the conditions (4.10). Therefore, the clustering in non-dominant component (baryons) on small scales can indeed be larger than that in dominant component (neutrinos).

However, Eq. (5.19) is correct only after the recombination, the above mentioned explanation is then available only if there were small scale perturbation in baryonic component and/or in massive neutrino component at the time of recombination as an initial fluctuation. Yet, such kind of initial fluctuations can be exist, because all the perturbations with scale smaller than $\lambda_{J\nu}$ in the neutrino component have already been erased at the time of recombination by collisionless Landau damping. Moreover, before the recombination, the Jeans length of baryon plus radiation component is much larger than $\lambda_{J\nu}$, it is also impossible to have any $\ell < \lambda_{J\nu}$ adiabatic perturbations in baryons at the recombination. Thus, in the neutrino dominant universe, we need to solve the difficulty of the lack of small scale perturbations at the recombination.

5.3 - Clustering Scenario in an Universe with two Kinds of Dark Matter^[30]

Both problems discussed in the last section might be

solved if the dark matter in the universe consists of two kinds of noninteracting particles, one is dominant component with larger velocity dispersion, such as massive neutrinos; one is non-dominant component which is more weakly interacting, more massive particle with smaller velocity dispersion. The candidates for the second kind of noninteracting particle might include the predicated gravitino, photino and right-handed neutrino.

The existence of different kinds of particles in the dark matter seems to be implied by the data on several dwarf spheroidal galaxies^[31]. It has been found that the mass-to-light ratio of Draco is roughly one order of magnitude larger than those of globular clusters. This means these dwarf galaxies possess a heavy halo of dark matter. The phase-space constraint in such small galaxies sets a lower limit of several hundred eV on the mass of the noninteracting particle if it is a kind of fermions^[32]. From the same data on dwarf spheroidal galaxies, one can also find a lower limit to the rest mass of particles in galactic halo to be about 3 eV^[33]. Therefore, only the properties of dwarf spheroidal galaxies already showed the varied components in dark matter.

Since more weakly interacting particles decoupled at higher temperature, its number density should be lower than neutrinos. Thus it is possible that the universe is still dominated by massive neutrinos, while the more massive particles are only to be a non-dominant component. The Jeans mass and length (or the free streaming length) of the more massive particle component are much smaller than that of neutrinos, for instance, the Jeans mass of $m = 1$ keV noninteracting particles can be equal to about $10^{12} M_{\odot}$. The Jeans length of the non-

-dominant component of dark matter λ_{Jg} is also shown in Fig. 7. It can be seen from Fig. 7 that in such a two component dark matter universe, the conditions (4.10) can also be satisfied before the recombination. Thus, small scale $\sim 10^{12} M_{\odot}$ perturbations can avoid to be erased by neutrino free streaming, and it can be kept in the non-dominant component until the recombination. Thus, the difficulty of the lack of small scale fluctuations at the recombination is solved and such small scale perturbations can also collapse before the formation of large scale structure.

Let us now consider the scenario of structure formation in the two component dark matter universe. Since in this model neutrino is still the dominant component, the picture of $\lambda \sim \lambda_{Jv}$ structure formation should be the same as that described in 5.1 and 5.2, namely, the large scale structure formed only at the time of $z \approx 2$. The picture for the small scale structure formation in two component dark matter model is quite different from the universe containing only one kind of dark matter. In the latter the small scale structure formed only after the large scale structure collapses, namely, the clustering process is from larger scales to smaller ones. The first objects to be condensed out would be that of mass about $10^{15} M_{\odot}$, then smaller scale objects such as galaxies form due to fragmentation. Thus, all the visible objects with small scales should have redshifts less than 2. However, in the two component dark matter model, it is possible to form small scale structure before the collapse of the large scale structure. According to the clustering feature under the conditions of (4.10), before the recombination, small scale clustering can take place in the non-dominant component of

dark matter; after the recombination, small scale clustering can take place in both the non-dominant dark matter and the baryons. These clustering processes are independent of the large scale clustering.

According to this clustering picture, there should be two kinds of visible objects with the scales less than super-clusters. One is to be formed by fragmentation of the large scale structure; one is not to link strongly with the formation of large scale structure. The distribution of the first kind of objects should have marked large scale inhomogeneity, while the second kind should have not such structure. Thus, this scenario leads to a testable prediction: the small scale objects with $z > 2$ should distribute more uniformly, especially on the scale of superclusters, than $z < 2$ objects. The test for this prediction will be discussed in the next section.

6. DISTRIBUTIONS OF OBJECTS WITH LARGE REDSHIFTS

6.1 - Large Scale Distribution of Quasars

The only known objects with redshift larger than 2 are quasars and intervening clouds implied by quasar absorption lines. Therefore, from the clustering scenario developed in 5.3, we could expect that:

- a) The distribution of quasars and intervening clouds should not have strong inhomogeneity as that of galaxies,
- b) The distribution of $z < 2$ quasars should be different from that of $z > 2$. The former has large scale clustering, while

the later has not.

The difficulty of to test these predictions is the lack of available samples of quasars. Most of homogeneous surveys for quasars listed only brighter quasars, or covered only very small area. These samples can not be used to do statistical analyses. Several wide field samples which are comparatively available for the tests are listed as follows:

- a) Savage and Bolton's survey of two $5^{\circ} \times 5^{\circ}$ fields near the South Galactic Pole^[34],
- b) CTIO optical quasar sample given by Osmer^[35],
- c) South Galactic Pole sample of Shanks et al.^[36],
- d) Smith and He's survey of a 40 quasars degree field centred at $01^{\text{h}}44^{\text{m}}$ and $-40^{\circ}00'$ ^[37].

An interesting investigation on the large scale clustering of the quasars listed in Savage-Bolton survey has been done by Chu and Zhu^[38]. The nearest neighbour test results are shown in Fig. 8 and 9, in which circular points show the distributions of nearest neighbour separation D from the Savage-Bolton's survey on the field $02^{\text{h}}, -50^{\circ}$. In Fig. 8 the histogram is the mean result of 10 Monte Carlo simulation generated by replacing the observed redshifts with random number, and in Fig. 9 by replacing the observed RA and DEC. The observed distribution is different, but rather small, from the Monte Carlo samples. They concluded that there is no clustering in the field $22^{\text{h}}, -18^{\circ}$ and the clustering is only of marginal significance in the field $02^{\text{h}}, -50^{\circ}$.

These results agree with the prediction a).

6.2 - Difference Between $z < 2$ and $z > 2$

The prediction of $z < 2$ and $z > 2$ quasars can also be tested by using the Savage-Bolton sample^[39]. Because which consists of two classes of quasars identified by different methods, i.e. the objective prism technique and the UV-B two colour method, the redshifts in this sample spreads on a more broad region than that of other surveys. It is then convenient to do the comparison between quasars of $z < 2$ and $z > 2$.

The results of the Nearest Neighbor Test are given in Table 2, in which N is the number of quasars, $\langle D_z \rangle$ denotes the sample's mean of nearest neighbor separation, D_z^* and $\hat{\sigma}$ are the mean and standard deviation for Monte Carlo samples, respectively. As a measure of the statistical significance, one define the following function

$$\delta = N^{1/2} \frac{\langle D_z \rangle - D_z^*}{\hat{\sigma}} \quad (6.1)$$

The distribution of δ is asymptotically normal with mean 0 and variance being 1. Therefore, $1 - p(\delta)$ in Table 2 is the probability that clustering is observed in the sample.

The main results from Table 2 are that an apparent clustering at 95% significant level for the sample of $z < 2$ in both fields, and there is no evidence of clustering for $z > 2$. These results can be more clearly seen in Figs. 10 and 11, in which the distributions of the nearest neighbor distance for each field are plotted. The observed $z < 2$ distributions (solid line) deviate obviously from the Monte Carlo samples (dashed line) on scale of 50 - 100 Mpc. It means that the distribution of $z < 2$ quasars does have ~ 100 Mpc clustering. The $z > 2$ distribution

does not show the difference from that of random sample, there is not distinguishable inhomogeneity.

The clustering of quasars in the sample of Shanks et al. [36] has been analysed by 2-dimensional correlation function method. They found that the UVX stars are clustered, while "probable" quasars identified by objective prism show no evidence of clustering. It is well known that the redshifts of quasars identified by UVB color method are smaller than 2, while by objective prism method are larger than about 1. Therefore, the difference of clustering between the UVX stars and the objective prism quasars can be seen as an evidence for the difference between $z < 2$ and $z > 2$ quasars.

Quasars listed in Smith-He catalog are identified by the objective prism method. By using power spectrum analysis, it is found no evidence for clustering of quasars in this catalog^[40]. CTIO sample is also given by the objective prism method. Most of the redshifts of quasars in this sample is of $z > 2$. Osmer already claimed no evidence for large scale clustering can be found from CTIO sample^[37,41].

A common result in these studies on large scale structure of quasars from different samples is that there are inhomogeneities on the scales of about 100 Mpc in the distributions of $z < 2$ quasars, but not of $z > 2$ quasars.

6.3 - Other Evidences for the Clustering Scenario^[42-43]

Binggeli pointed out^[44] that the major axis of a cluster tends to point to the nearest neighbor cluster. If the

distance between a cluster and its nearest neighbor is less than 35 Mpc, the angle between the major axis of the cluster and the direction to the nearest neighbor is always smaller than 45° . No such correlation exists if the nearest neighbor distance is larger than 35 Mpc. Therefore, the orientation correlation is also an evidence of large scale inhomogeneity in the distribution of clusters.

A similar study for radio double sources has been done recently^[45]. Using a complete sample of radio double sources by Condon et al.^[46], one found some statistical evidences of the correlation between the orientation of the double sources and the direction to their nearest neighbor radio sources, the correlation scale is also on about tens Mpc, but the correlation is not so obvious as that of clusters of galaxies. Not all of radio double sources are quasars. Since these sources are selected by the criterion of the separation between two components to be less than 1.5 arcmin, many of them should probably be quasars.

The Ly- α absorption lines in quasar spectrum might indicate the locations of intergalactic clouds. The redshift distribution of Ly- α absorption lines should then show the clustering of intergalactic clouds. Sargent et al. studied^[47] six quasars with very rich absorption lines, the redshifts of which cover from 1.7 to 3.3. They did not find any evidence of the inhomogeneity in the absorption line distribution. By using different method, which is especially available to analyse the inhomogeneity with scale of a few hundreds Mpc, it is found^[48] that the absorption lines distribute inhomogeneous, but the amplitude of the inhomogeneity is very small.

An evidence for the difference between $z < 2$ and

and $z > 2$ quasars has also been found from the research on the evolution of optically selected quasars. Veron^[49] have built the luminosity function of quasars at various redshifts, using the number-magnitude relation for quasars and the redshift distributions at various apparent magnitude. He found that the evolution law for small redshift is quite different from that for large one; the evolution is very fast for $1 < z < 2.3$, while at some $z > 2.3$ the evolution has to stop and even to reverse. This shows again that $z \approx 2$ is a crucial time of the large scale structure formation.

TABLE 1

Inhomogeneities in the present universe.

Objects	Size	Mass	δ
galaxies	50 kpc	$\sim 10^{12}$ M	$\sim 10^3$
cluster of galaxies	5 Mpc	$\sim 10^{14}$ M	1 - 10
superclusters	30 - 100 Mpc	$\sim 10^{15}$ M	~ 1
voids	100 Mpc		

TABLE 2

Nearest neighbor test.

Redshift	N	Quasar data $\langle D \rangle$ Mpc	Monte Carlo data D^* Mpc	$\bar{\sigma}$	δ	1 - P(δ)
(02 ^h , -50 ^o)						
z < 2	62	141.7	159.0	79.6	-1.72	96%
z > 2	48	201.0	205.9	83.2	-0.40	66%
(22 ^h , -18 ^o)						
z < 2	57	146.7	165.8	77.9	-1.84	97%
z > 2	26	207.1	193.0	75.9	> 0	-

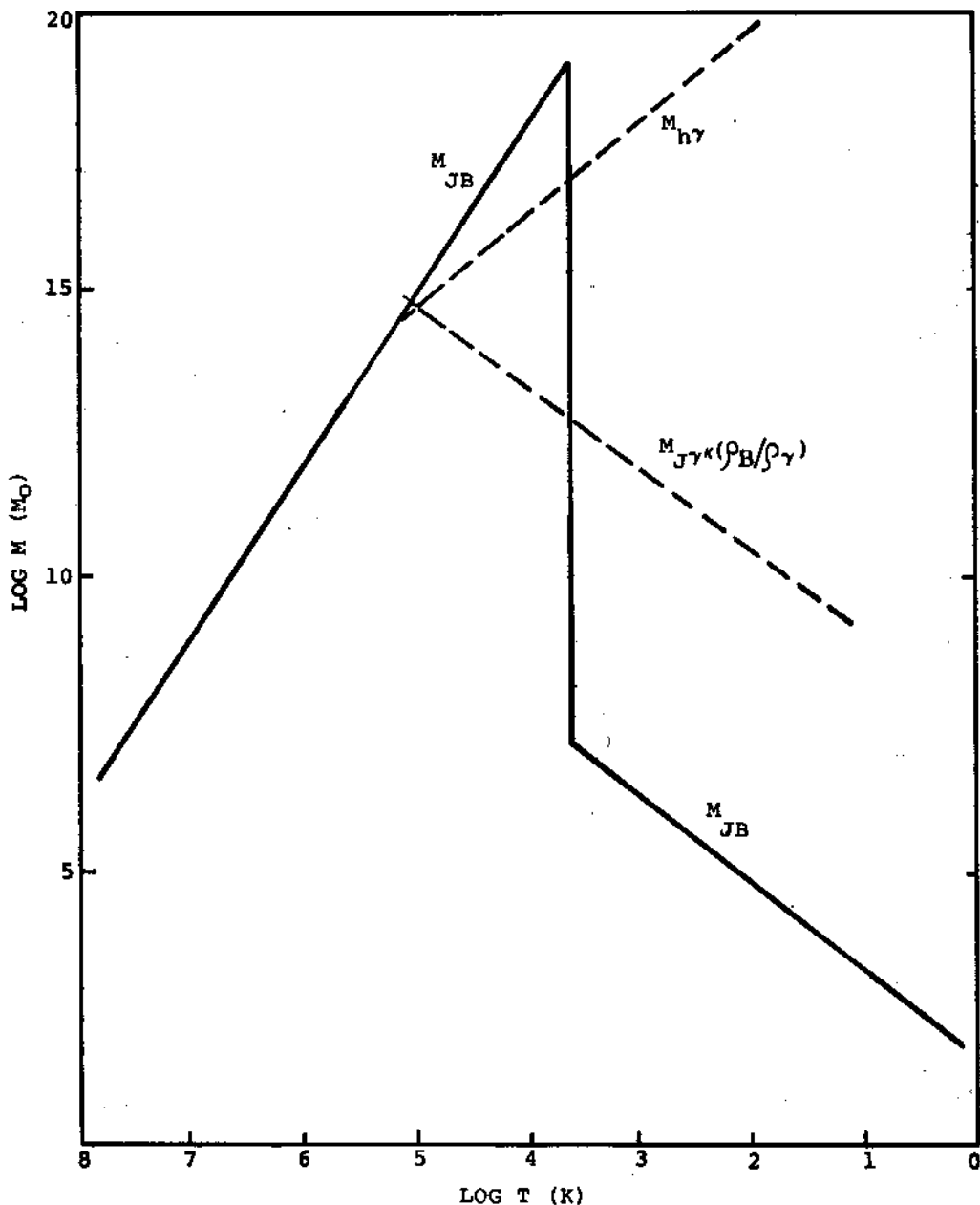


FIG. 1 Jeans mass as a function of the cosmic temperature. The solid line corresponds to the case of the universe containing only baryons and radiation, the dashed line to the neutrino dominant universe. Line $M_{h\gamma}$ gives the mass contained within the particle horizon.

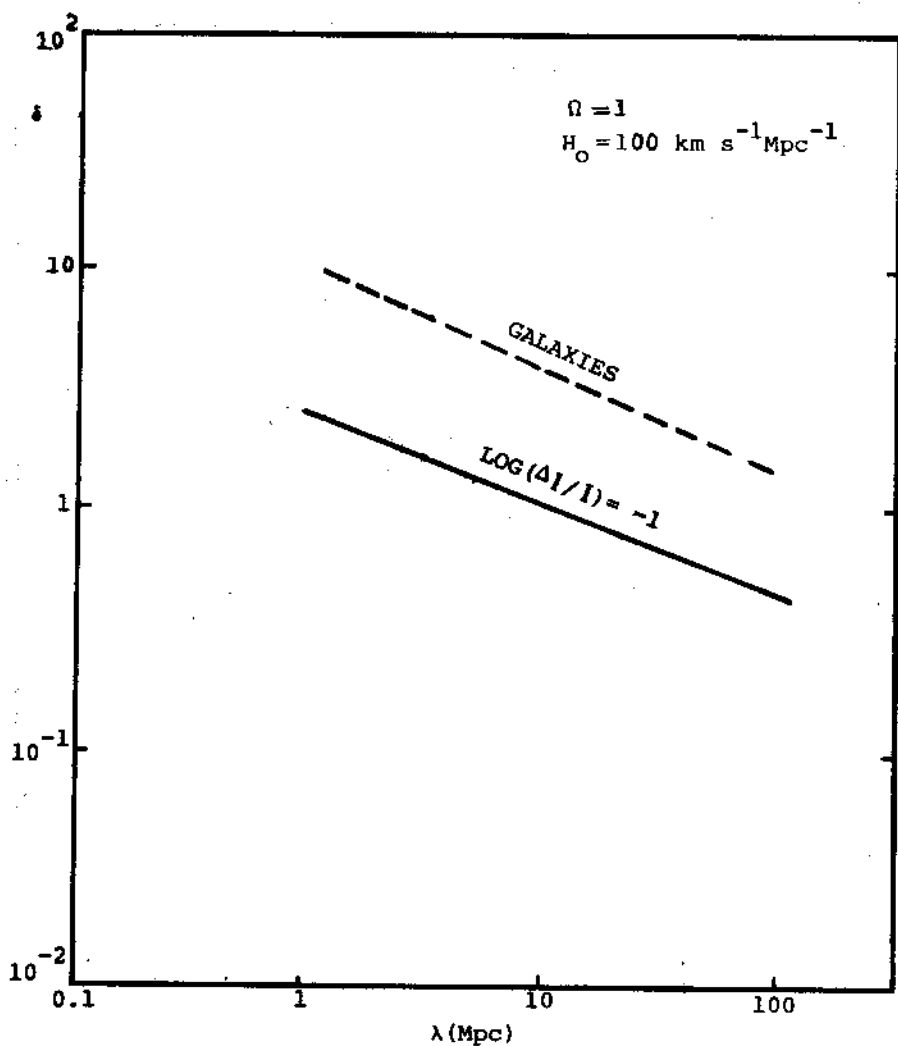


FIG. 2 Upper limit to the inhomogeneity given by the quasar's luminosity fluctuation of gravitational lensing effect.

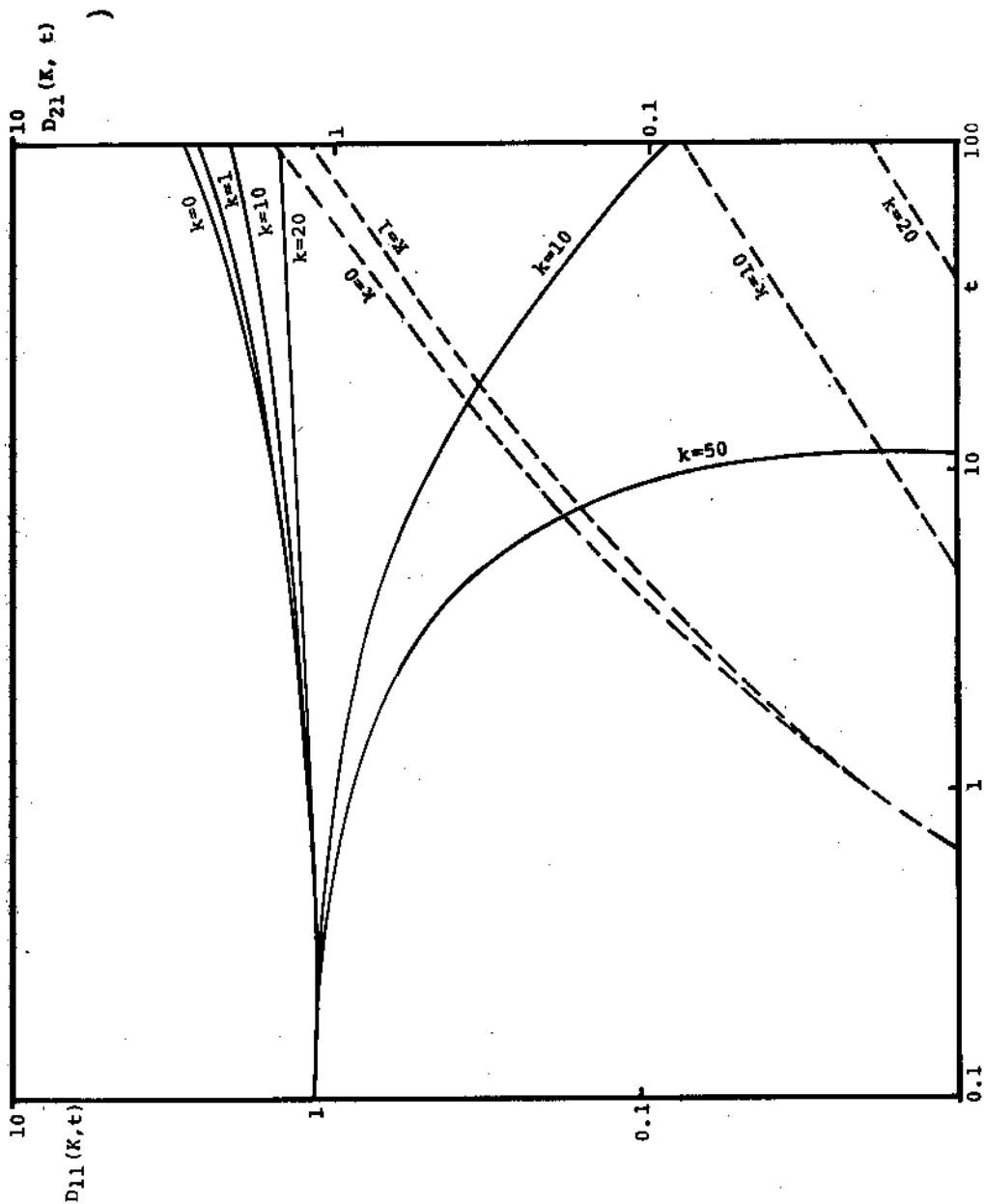


FIG. 3 The development matrix elements of $D_{11}(k,t)$ (solid lines) and $D_{21}(k,t)$ (dashed lines), which are equal, respectively, to $\delta_{1k}(t)$ and $\delta_{2k}(t)$ in the case of initial perturbation $\delta_{1k}(0) = 1$ and $\delta_{2k}(0) = 0$.

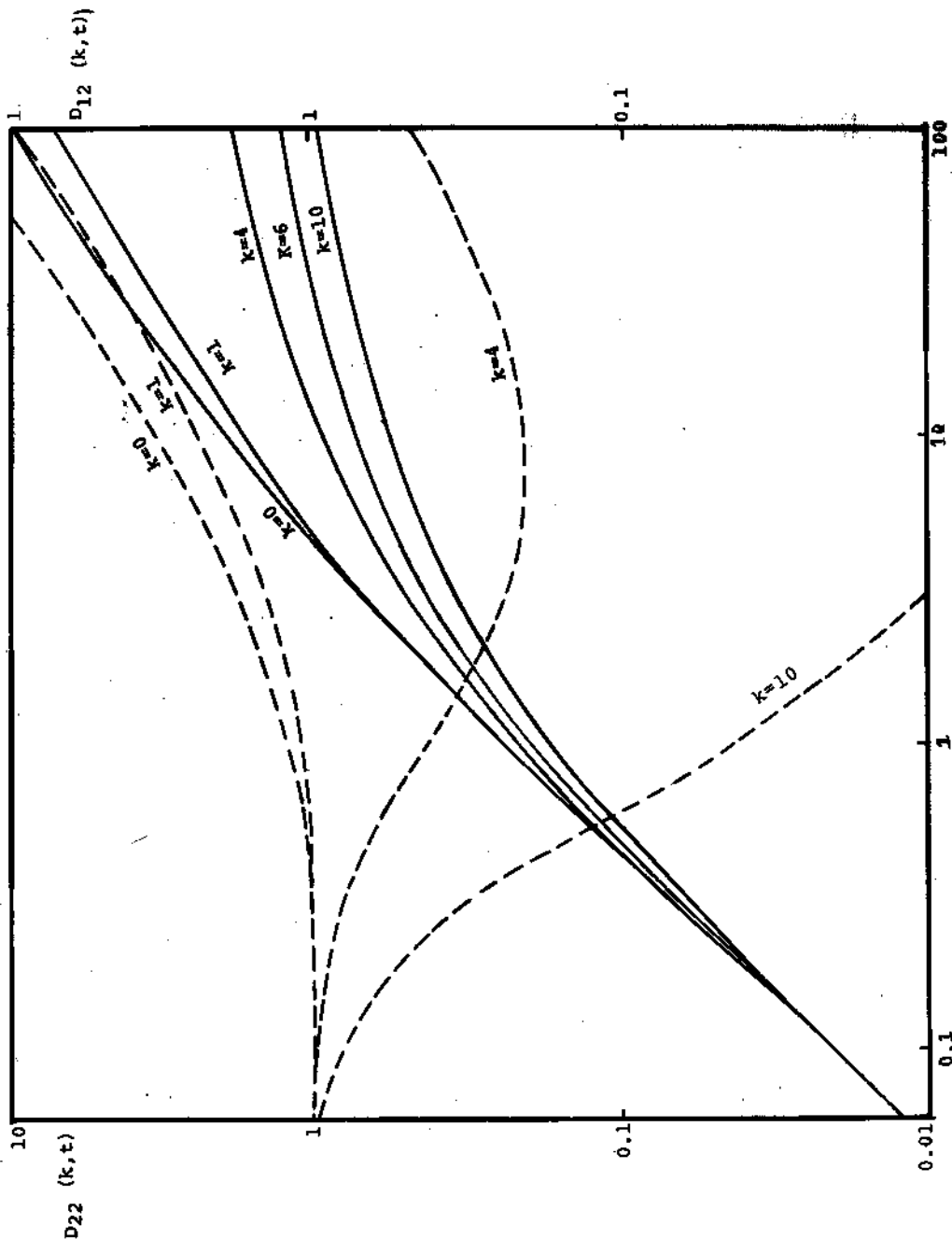


FIG. 4 The development matrix elements of $D_{22}(k,t)$ (dashed lines) and $D_{12}(k,t)$ (solid lines), which are equal, respectively, to $\delta_{2k}(t)$ and $\delta_{1k}(t)$ in the case of initial perturbation $\delta_{2k}(0) = 1$ and $\delta_{1k}(0) = 0$

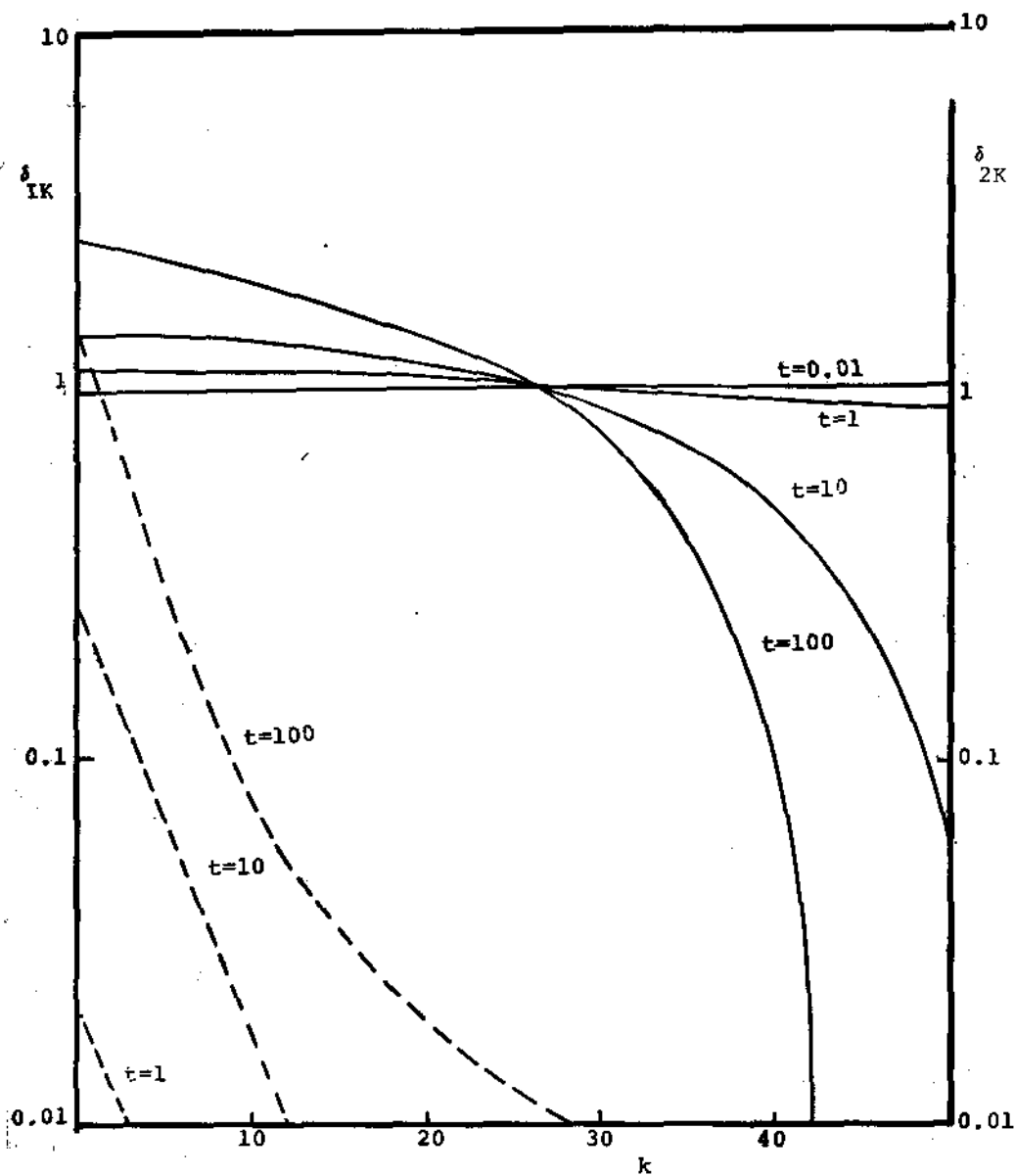


FIG. 5 Evolution of the spectrum of inhomogeneities in non-dominant component (solid lines) and in dominant component (dashed lines) in the case of initial perturbation $\delta_{1k}(0) = 1$ and $\delta_{2k}(0) = 0$.

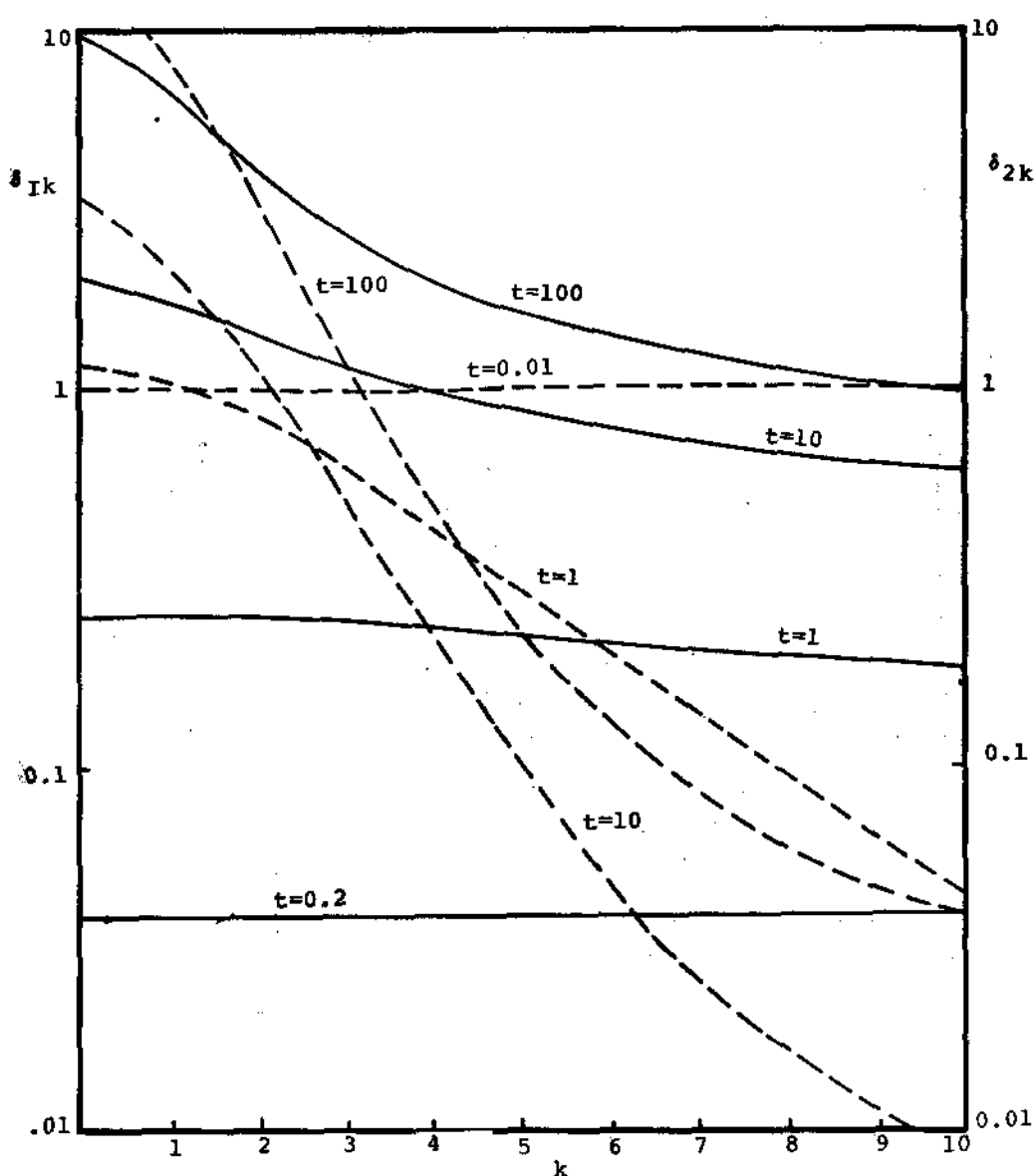


FIG. 6 Evolution of the spectrum of inhomogeneities in dominant component (dashed lines) and in non-dominant component (solid lines) in the case of initial perturbation $\delta_{1k}(0) = 0$ and $\delta_{2k}(0) = 1$.

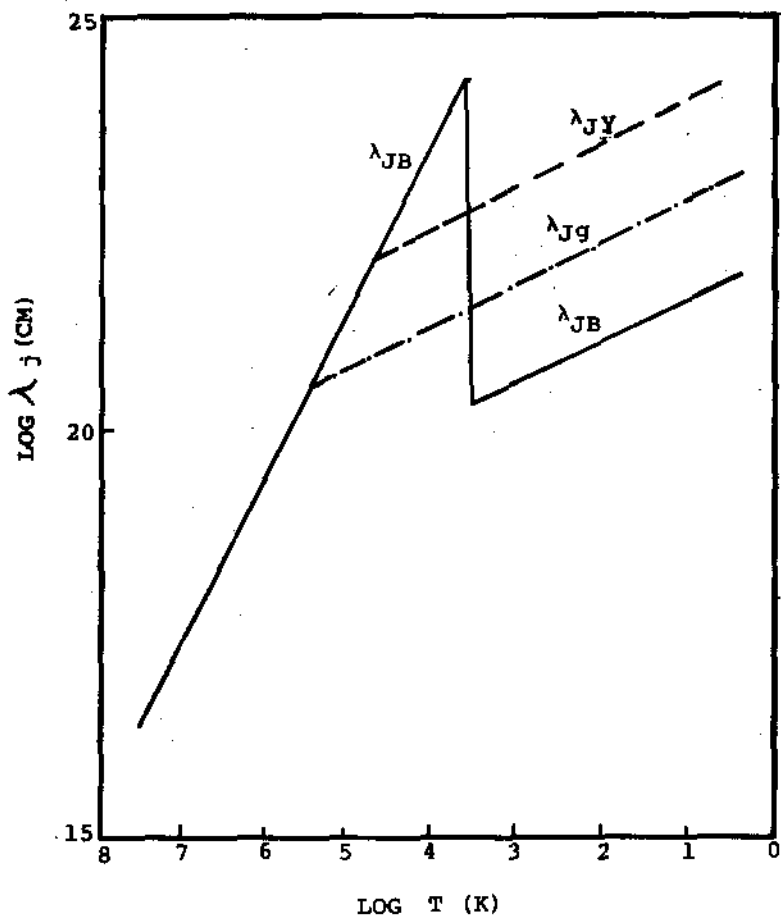


FIG. 7 Jeans length as a function of the cosmic temperature. The solid line corresponds to the case of the universe containing only baryons and radiation; dashed line to the massive neutrino component; dot-dashed line to the non-dominant component of dark matter.

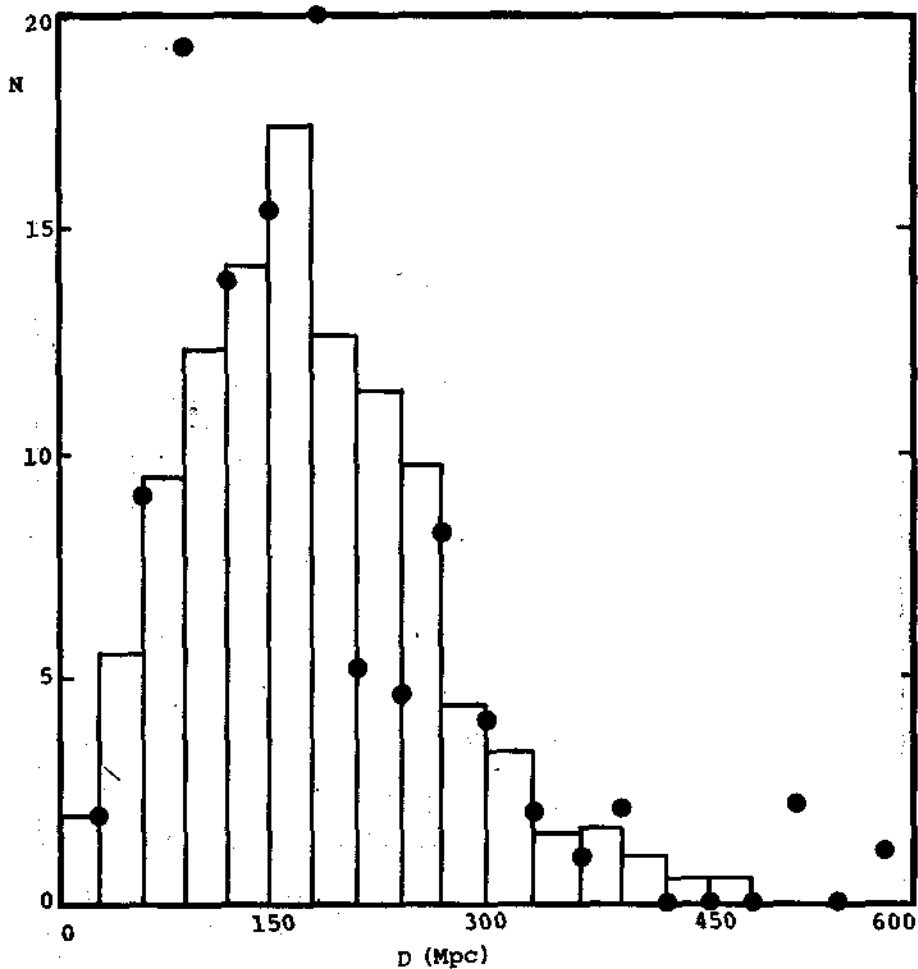


FIG. 8 Nearest neighbor test for quasar distribution. Circular points are from the observed results of Savage-Bolton survey on the field $02^{\text{h}}, -50^{\circ}$. Histogram is the mean of 10 Monte Carlo simulations by randomizing z .

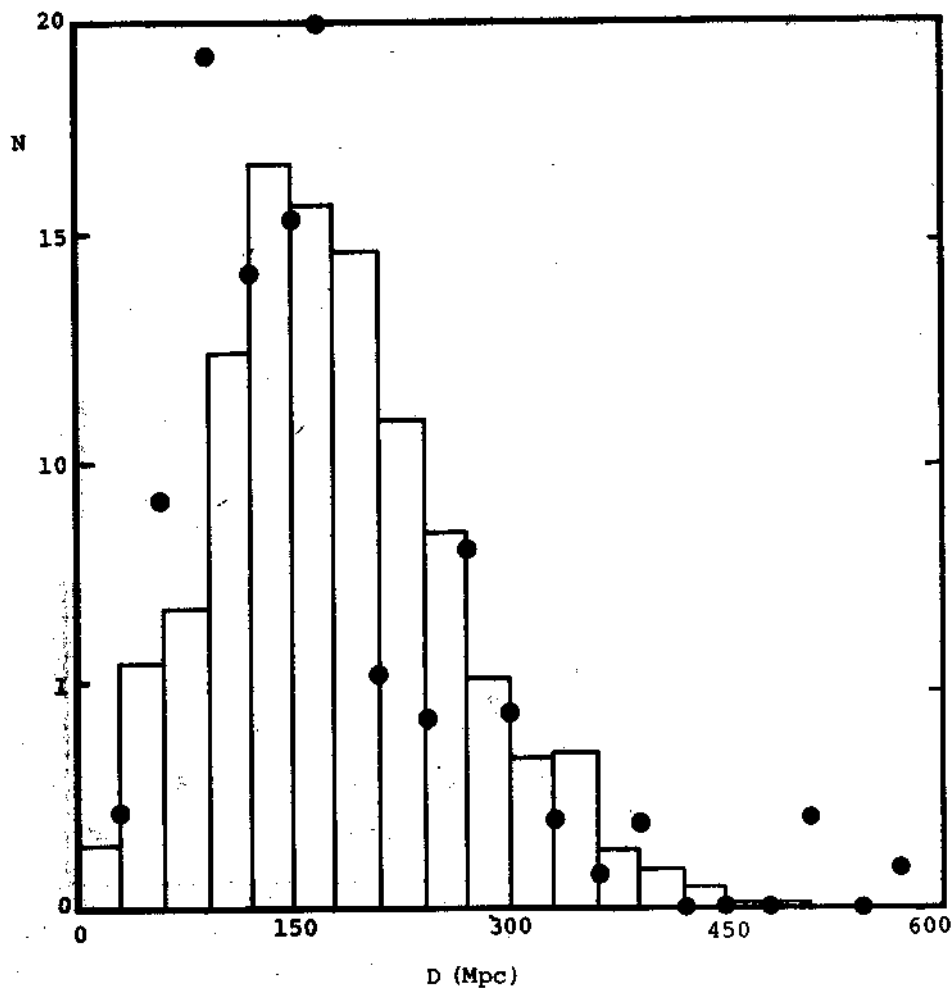


FIG. 9 The same as Fig. 8, but by randomizing RA and DEC.

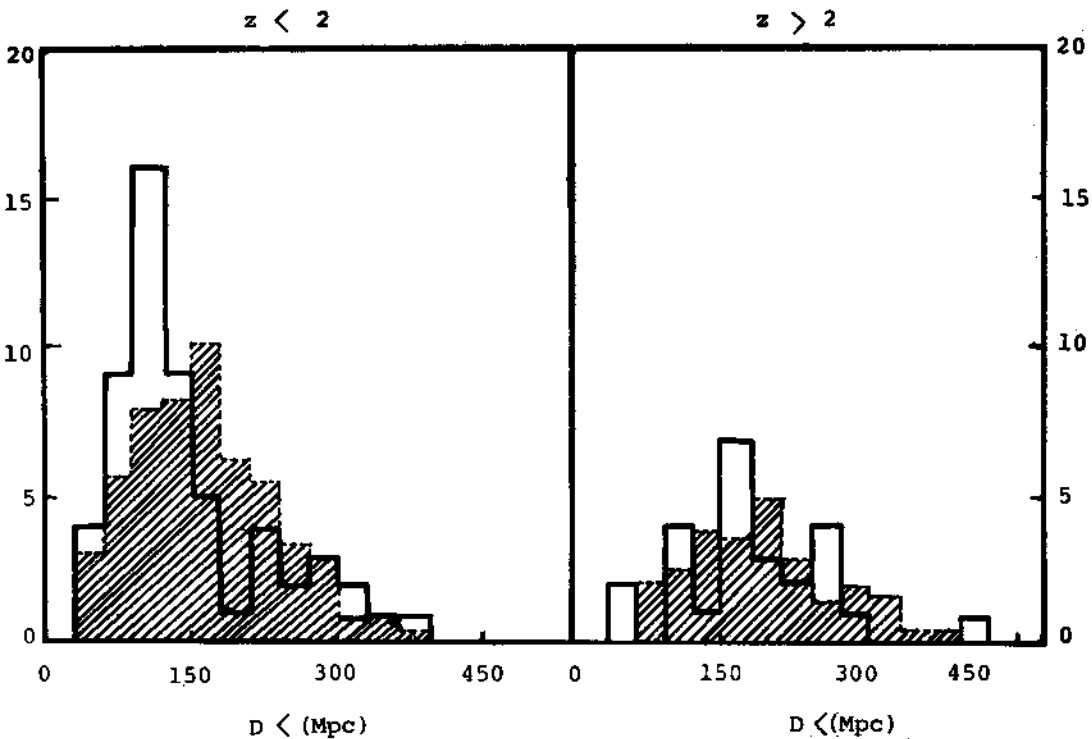


FIG. 10 The distribution of nearest neighbor distance for $z < 2$, $z > 2$ in the field $02^h, -50^\circ$ of Savage-Bolton survey (solid line). Dashed line corresponds to the mean of 10 Monte Carlo simulation.

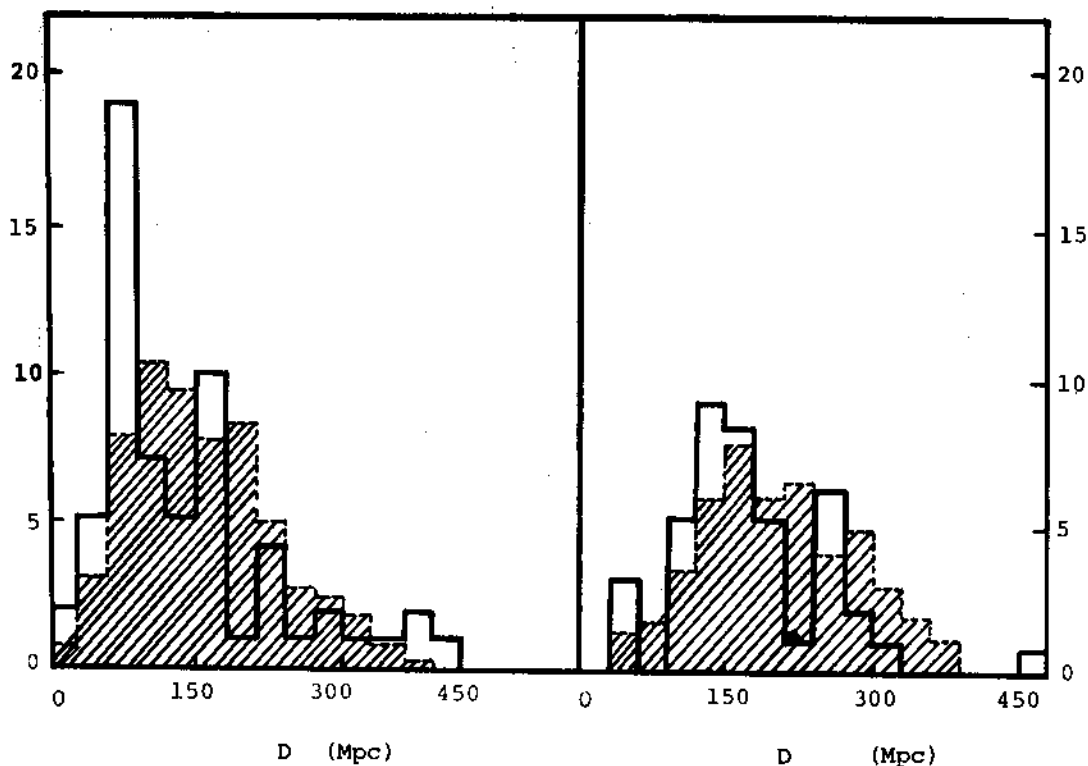
$z < 2$ $z > 2$ 

FIG. 11 The same as Fig. 10, but for quasars in the field $22^{\text{h}}, -18^{\circ}$.

References

- [1] J.H. Oort, *An. Rev. Astr. Astrophys.*, 21(1983)373.
- [2] Ya. B. Zeldovich, J. Einasto and S.F. Shandarin, *Nature*, 300 (1982) 407.
- [3] L.Z. Fang and R. Ruffini, *Basic concepts on relativistic astrophysics*, World Scientific, Singapore, 1983.
- [4] S. Weinberg, *Gravitation and Cosmology*, John Wiley & Sons, New York, 1972.
- [5] E.W. Kolb and M.S. Turner, *Ann. Rev. Nucl. Part. Sci.*, 33 (1983)645.
- [6] J.M. Uson and D.T. Wilkinson, *Astrophys. J. Lett.*, 277(1984) L1.
- [7] V.C. Rubin, *Internal Kinematic and Dynamics of Galaxies*, ed. E. Athanassoula, Reidel, Dordrecht, 1983.
- [8] S.M. Faber & J.S. Gallagher, *Ann. Rev. Astr. Astrophys.*, 17 (1979)135.
- [9] L.Z. Fang, T. Kiang, F.H. Cheng and F.X. Hu, *Quarterly J. of R.A.S.*, 23(1982)363.
- [10] A.H. Guth, *Phys. Rev.*, D23(1981)347.
- [11] L.Z. Fang, *Cosmology of the early universe*, eds. L.Z. Fang and R. Ruffini, World Scientific, Singapore, 1984.
- [12] G. De Vaucouleurs and G. Bollinger, *Astrophys. J.*, 233 (1979) 433.
- [13] J. Mould, M. Aaronson and J. Huchra, *Astrophys. J.*, 238 (1980)458.
- [14] A. Yshil, A. Sandage and G.A. Tammann, *Astrophys. J.*, 242 (1980)448.
- [15] S.M. Fall, *Mon. Not. R. Astr. Soc.*, 172(1975)23p.
- [16] M. Davis and P.J.E. Peebles, *Astrophys. J. Suppl.*, 34(1977) 425.

- [17] M.J. Geller and M. Davis, *Astrophys. J.*, 225(1978)1.
- [18] L.Z. Fang and H. Sato, *Prog. Theor. Phys.* 67(1982)1994.
- [19] L.Z. Fang, Proceedings of the third Marcel Grossman Meeting on general relativity, ed. Hu Ning, Science Press and North-Holland Publishing Co., 1983.
- [20] L.Z. Fang, Y. Q. Chu and X.F. Zhu, in prep.
- [21] L.Z. Fang, Clusters and Groups of galaxies, eds. F. Mardirossian, G. Giuricin and M. Mezzetti, Reidel, Dordrecht, 1984.
- [22] M. Guyot and Ya. B. Zeldovich, *Astr. Astrophys.*, 9 (1970) 227.
- [23] P. Meszaros, *Astr. Astrophys.*, 37(1974)225.
- [24] I. Wasserman, *Astrophys. J.*, 248(1981)1.
- [25] L.Z. Fang and Y.Z. Liu, *Lett. Nuovo Cimento*, 32(1981)129.
- [26] I.H. Gilbert, *Astrophys. J.*, 144(1966)233.
- [27] T. Lu and L.Z. Fang, Proceedings of the third Marcel Grossmann Meeting on general relativity, ed. Hu Ning, Science Press and North-Holland Publishing Co., 1983.
- [28] C. Frenk, S.D.M. White and M. Davis, *Astrophys. J.*, 271 (1983)417.
- [29] N. Kaiser, *Astrophys. J.*, 273(1983)L17.
- [30] L.Z. Fang, S.X. Li and S.P. Xiang, *Astr. Astrophys.*, in Press.
- [31] S.M. Faber and D.N.C. Lin, *Astrophys. J. Lett.*, 266(1983)L17.
- [32] D.N.C. Lin and S.M. Faber, *Astrophys. J. Lett.*, 266(1983)L21.
- [33] L.Z. Fang and J.G. Gao, *Phys. Lett.*, 139B(1984)351.
- [34] A. Savage and J.G. Bolton, *Mon. Not. R. Astr. Soc.*, 188(1979)599.
- [35] P.S. Osmer, *Astrophys. J.*, 247(1981)761.
- [36] T. Shanks, R. Fong, M.R. Green, R.C. Clowes and A. Savage, *Non. Not. R. Astr. Soc.*, 203(1983)181.
- [37] M.G. Smith and X.T. He, preprint.
- [38] Y.Q. Chu and X.F. Zhu, *Astrophys. J.*, 267(1983)4.

- [39] L.Z. Fang, Y.Q. Chu and X.F. Zhu, *Scientia Sinica*, in Press.
- [40] X.T. He, Y.Q. Chu, L.Z. Fang and M.G. Smith, in prep.
- [41] A. Webster, *Mon. Not. R. Astr. Soc.*, 199(1982)683.
- [42] L.Z. Fang, *Astrophysical Cosmology: Proceedings of the Study Week on Cosmology and Fundamental Physics*, eds. H. A. Brück, G.V. Coyne and M.S. Longair, Pontifical Scientific Academy, Vatican, 1982.
- [43] L.Z. Fang, Y.Q. Chu, Y.Z. Liu and C.L. Cao, *Astr. Astrophys.* 106(1982)287.
- [44] B. Binggeli, *Astr. Astrophys.*, 107(1982)338.
- [45] L.Z. Fang, Y.Q. Chu and X.F. Zhu, *Astr. Astrophys.*, in press.
- [46] J.J. Condon, M.A. Condon and C. Hazard, *Astr. J.*, 87 (1982) 739.
- [47] W.L.W. Sargent, P.J. Young, A. Boksenberg and D. Tytler, *Astrophys. J. Suppl.*, 42(1980)41.
- [48] Y.Q. Chu, L.Z. Fang and Y.Z. Liu, *Astrophys. Lett.*, (1984).
- [49] P. Veron, *Quasars and Gravitational Lenses*. 24th Liege Astrophysical Colloquium, Institut d'Astrophysique, 1983.